The impact of curcumin derived polyphenols on the structure and flexibility COVID-19 main protease binding pocket: A molecular dynamics simulation study

Aweke Mulu [Corresp., 1] , Mulugeta Gajaa [2] , Haregewoin Bezu Woldekidan [1] , Jerusalem Fekadu W/mariam [1]

[1] College of APPLIED SCIENCE, ADDIS ABABA SCIENCE AND TECHNOLOGY, ADDIS ABABA, Non-US/Non-Canadian, Ethiopia

[2] College of Natural and Social science, ADDIS ABABA SCIENCE AND TECHNOLOGY, ADDIS ABABA, Non-US/Non-Canadian, Ethiopia

Corresponding Author: Aweke Mulu
Email address: aweke.mulu@aastu.edu.et

The newly occurred SARS-CoV-2 caused a leading pandemic of coronavirus disease (COVID-19). Up to know it has been infected more than one hundred sixty million and killed more than three million people according to 14 May 2021 World Health Organization report. So far, different types of studies have been conducted to develop anti-viral drug for COVID-19 with no success yet. As part of this, silico studies used to discover and introduce COVID-19 antiviral drugs and results showed that protease inhibitors could be very effective in controlling. The aim of this study is to investigate the binding affinity of three curcumin derived polyphenols against COVID-19 the main protease (Mpro), binding pocket and identification of important residues for interaction. In this study, molecular modeling, auto-dock coupled with molecular dynamics simulations was performed to analyze the conformational and stability of COVID-19 binding pocket with diferuloylmethane, demethoxycurcumin and bisdemethoxycurcumin. All three compounds has showed binding affinity -39, -89 and −169.7, respectively. Demethoxycurcumin and bisdemethoxycurcumin showed optimum binding affinity with target molecule and these could be one of potential ligands for COVID-19 therapy. And also, COVID-19 main protease binding pocket binds with the interface region by one hydrogen bond. Moreover, the MD simulation parameters indicated that demethoxycurcumin and bisdemethoxycurcumin were stable during the simulation run. These findings can be used as base line to develop therapeutics with curcumin derived polyphenols against COVID-19.

1 The impact of curcumin derived polyphenols on the structure and flexibility
2 COVID-19 main protease binding pocket: A molecular dynamics simulation study

3 Aweke Mulu Belachew[1*], Mulugeta Gajaa Ufgaa[2], Haregewoin Bezu Woldekidan[3] and
4 Jerusalem Fekadu W/ Mariam [4]

5 [1,3,4] College of Applied Science, Addis Ababa Science and Technology University, Addis Ababa,
6 Ethiopia
7 [2] College of Natural and Social science, Addis Ababa Science and Technology University, Addis
8 Ababa, Ethiopia
9 Corresponding Author:

10 Aweke Mulu Belachew[1*]

11 Addis Ababa, Ethiopia, 16417, Ethiopia

12 Email address: aweke.mulu@aastu.edu.et

13 **Abstract**

14 The newly occurred SARS-CoV-2 caused a leading pandemic of coronavirus disease (COVID-
15 19). Up to know it has been infected more than one hundred sixty million and killed more than
16 three million people according to 14 May 2021 World Health Organization report. So far,
17 different types of studies have been conducted to develop anti-viral drug for COVID-19 with no
18 success yet. As part of this, silico studies used to discover and introduce COVID-19 antiviral
19 drugs and results showed that protease inhibitors could be very effective in controlling. The aim
20 of this study is to investigate the binding affinity of three curcumin derived polyphenols against
21 COVID-19 the main protease (Mpro), binding pocket and identification of important residues for
22 interaction. In this study, molecular modeling, auto-dock coupled with molecular dynamics
23 simulations was performed to analyze the conformational and stability of COVID-19 binding
24 pocket with diferuloylmethane, demethoxycurcumin and bisdemethoxycurcumin. All three
25 compounds has showed binding affinity -39, -89 and −169.7, respectively. Demethoxycurcumin
26 and bisdemethoxycurcumin showed optimum binding affinity with target molecule and these
27 could be one of potential ligands for COVID-19 therapy. And also, COVID-19 main protease
28 binding pocket binds with the interface region by one hydrogen bond. Moreover, the MD
29 simulation parameters indicated that demethoxycurcumin and bisdemethoxycurcumin were
30 stable during the simulation run. These findings can be used as base line to develop therapeutics
31 with curcumin derived polyphenols against COVID-19.

32 **Keywords:** NAMD; X-ray crustal structure; SARS-CoV-2; Docking; binding energy

Introduction

The severe acute respiratory syndrome coronavirus 2 (SARS-CoV-2), which was first reported in Hubei Province of Wuhan, China in December 2019, is responsible for the ongoing global pandemic of coronavirus disease 2019 (COVID-19) spreading across almost all countries with 160 686 749 active infection cases and 3335 948 deaths until 14   May 2021 [1 2 10]. The actual number of cases presumed much higher, due to limitation in testing, lack of medication, and applying World Health Organization recommendation such as, social distancing, hand washing, and travel ban and full lockdown in many cities [1 3 10]. Prior work in this area showed that ⁃ SARS-CoV-2 is the third coronavirus belonging to Genus Beta coronavirus that can infect human next coronavirus-severe acute respiratory syndrome (SARS-CoV-2) and the Middle East respiratory syndrome (MERS-CoV) [2]. SARS-CoV-2, the virus responsible for COVID-19, belongs to a group of genetically related viruses that includes SARS-COV and a number of other CoVs isolated from bat populations [1]. The SARS-CoV-2 virus is the primary causative agent of COVID-19. The pol gene of the SARS-CoV-2 virus possesses a positive-sense ~30kb long RNA genome with ~14 ORFs and encoding 27 proteins [3 39]. Among multiple encoded proteins Programmed ribosomal frame shifting generates two polyproteins encoding the replicase proteins [4]. Range of viral processing protein associated with structural proteins, non-structural proteins, and accessory proteins have been reported in several studies [1 4 5]. The pol gene of the SARS-CoV-2 virus encodes two protease enzymes main protease (Mpro) and Papain-like protease, which are involved in the proteolytic processing of the polyproteins into individual nsp7/nsp8/nsp12 to control viral gene expression and replication in the host [3 4 5]. SARS-CoV-2 virus Mpro is a vital enzyme that catalyzes the proteolytic process, non-structural proteins (nsps) generated by the main protease play a major role in the reverse-transcribed viral DNA into the host genome [4 6 44 45]. It is composed of three structurally and functionally distinct domains: domain I, II, and III. Domain I and II contain highly conserved Cys145-His41 residues located in the cleft which are directly involved in the catalytic activities of Mpro [7]. Therefore, SARS-CoV-2 virus Mpro has emerged as a promising antiviral target as this is responsible for newly synthesized double-stranded viral DNA and subsequent maturation of polyproteins into host genomic DNA. SARS-CoV-2 virus Mpro inhibitors repurposing, which target the enzyme active site, have been studied computationally over the past few months to control COVID-19 as there is an urgent requirement for a strong drug or combination of drugs to combat the pandemic

64   [8 9]. Currently, natural product are screened by molecular docking and molecular dynamic

65   simulation to test their affinity towards molecular targets of COVID-19 taking the advantage that

66   natural products are free from toxic or side effects [44 46 47]. In this study, the structure of

67   SARS-CoV-2 virus Mpro was obtained from the protein data bank (PDB) gave a major advance

68   for structure-based drug design of Curcumin derivative polyphenols, and gives well-established

69   techniques to reveal important dynamic information in proteins. This is an exciting new approach

70   to develop effective therapies to fight COVID-19 with Curcumin, exploiting a new mechanism

71   based on well-validated virulence factors. And also, expanding the list of lead compounds means

72   more possible drugs that could be advanced through clinical trials and better treatments will be

73   possible shortly.

74   Up to now, there are no robust drugs for the wide-spread SARS-CoV-2 virus although there are

75   now several vaccines that are in use. Finding a new drug in a wet lab and bringing it to market is

76   hard, expensive, and time-consuming. Due to rapid ongoing global health emergency in the

77   current outbreak and high mortality rate estimated by World Health Organization, the more rapid

78   development of new antiviral drugs is highly demanded [10 39]. In the literature, traditional

79   medicines have been extensively investigated to find novel therapeutic strategies for viruses

80   including SARS-CoV-2. Evidence from several computational studies indicated that natural

81   compounds for virus infection treatment play a critical role. A review of the literature showed

82   that natural compounds with low cytotoxicity and high bioavailability seem to be the most

83   efficient candidate's therapy. And also, studies observed lining modern medicine, humans have

84   relayed to the use of phytochemicals for the treatment of different diseases [11 12]. In general

85   work to date in this area supports phytochemicals such as polyphenols possessing a variety of

86   potential biological benefits such as Anti-oxidant, Anti-inflammatory, antiviral, and antibacterial

87   [13 14]. A systematic review of peer-reviewed literature showed that Curcumin has antiviral

88   activity in human immunodeficiency virus, herpes simplex virus, dengue virus, Zika, and

89   chikungunya viruses [13 14 15 16]. The main objective of this work is to investigate methods for

90   improving Curcumin derivative polyphenols that will be required for developing Mpro inhibitors

91   were performed with silico study that included molecular docking combined with molecular

92   dynamic simulation depend on Mpro binding pocket (PDB ID: 7BUY) [7]. Specifically, we aim

93   to investigate the amino acids that contribute the most to the binding Curcumin-derived

94   polyphenols; we examined the binding mode of the Mpro pocket and found that form hydrogen

95   bonds with binding pocket of residues. Finally, we put into MD simulation and binding free

96   energy calculation. Results revealed that demethoxycurcumin and bisdemethoxycurcumin

97   (especially bisdemethoxycurcumin), could have good inhibitory activity towards Mpro.

98   **Materials & Methods**

99   Protein and Polyphenols Structure Preparation

100   The crystal structure of the MPro: carmofur complex (PDB ID: 7BUY) [7] was retrieved from

101   the Protein Data Bank (PDB). A high-quality homology model of Apo-enzyme (without

102   carmofur) was calculated using MODELLER version 9.10 [25]. Before docking, crystallographic

103   water molecules and bound ligands were removed from 3D structures. The protonation states of

104   acidic and basic residues were determined under pH 7.0 conditions and analyzed by the H++

105   server [17]. Next, the Modell structure was subjected to Discovery studio for optimization and

106   minimization. Finally, validate the modeled structure using the UCLA-DOE server

107   (http://servicesn.mbi.ucla.edu/) [18 19 20]. The modeled 3D structure was then validated and

108   confirmed by using the RAMPAGE, ERRAT, and Verify3D online servers. After validating the

109   homology models, we resolved the issue of mismatched residue and missed structure across the

110   two models. The SMILES of the three natural polyphenols diferuloylmethane,

111   demethoxycurcumin, and bisdemethoxycurcumin were obtained from Pub Chem [21] and their

112   accession numbers are DB969516, DB5469424, and DB5315472 respectively. These SMILES

113   were converted to PDB format with 3 D coordinates using Open Babel [22], an open-source

114   chemical toolbox for the inter conversion of chemical structures.

115   Docking Methodology

116   The experiments were performed with Auto-Dock 4.2 according to the previous study procedure

117   [23]. The work was separated into two parts; the first was prepared ligand and protein pdbqt file

118   and Docking Parameter file using Auto-Dock 4.2. The second was performed molecular docking

119   and finally, the results were analyzed. Fourteen refined 3D polyphenols structures were screened

120   for binding affinity and selectivity toward protein. To cover the whole protein structure global

121   docking was conducted with the spacing of 0.5 Å. Subsequently, rigid or flexible docking of the

122   target was performed and then the complexes with the lowest binding energies are selected. The

123   genetic algorithm was used to evaluate parameters with the default setting, and Lamarckian GA

124   (4.2) was employed for docking simulations. All docking parameters procedures were set to 150

125 genetic algorithm runs using the Lamarckian genetic algorithm conformational search, with the

126 population size of 300, 2500000 maximum numbers of energy evaluations, and 27000

127 generations per run. The best protein-polyphenols complexes were selected according to the

128 molecular docking results including binding energy, root mean square deviation, and type of

129 favorable interactions and binding sites.

130 Set Simulation Parameters and Molecular Dynamics

131 To explore the conformational flexibility of best hit compounds against free protein, an MD

132 simulation study was employed using NAMD 2.3 tool on window operating system [24]. Each

133 complex was separated for generating topology and coordinates. The protein topology and

134 coordinate files were lacking in the Amber force field prepared by the general amber force field

135 (CgenFF) Server [25], while the ligands topology and coordinate files were generated using

136 Open Babel [22]. The generated NAMD compatible files for the proteins and the ligands were

137 then merged, and then complex subjected to solvated, minimized, and equilibrated. The systems

138 were solvated in a cubic water-box with the explicit solvation model TIP3P.20 we used a

139 distance of 1.0 Å between the cell wall and the solvated atoms of the system. Counter-ions were

140 also added to neutralize the system. The energy minimization (n steps = 5000) was conducted

141 using the steepest descent approach (1000ps) for each protein-ligand complex. Particle Mesh

142 Ewald (PME) method was employed for energy calculation and for electrostatic and Van der

143 Waals interactions; cut-off distance for the short-range Van der Waals was set to 10 Å, where

144 Coulomb cut-off and neighbor list were fixed at 8 Å. Finally, a 50ns molecular dynamics

145 simulation was carried out for all the complexes with n steps 1000000. The RMSD, hydrogen

146 bond distribution, and RMSF analysis were carried out using MS Excel (2016), VMD, and

147 UCSF Chimera 1.10.1 software. Trajectory snapshots were stored at every 0.2ps during the

148 simulation period, and 3D coordinate files were harvested after every 2fs for post-dynamic

149 analysis.

150 MM-PBSA Approach Interaction energy

151 The binding energy of Mpro-Curcumin derivative polyphenols complexes was calculated using

152 the molecular mechanics Poisson–Boltzmann surface area (MM-PBSA) method [26]. Free

153 energy of solvation (TP3 solvent model) and molecular mechanics potential energy was

154 calculated. In this study, snapshots were taken from MD simulation used for calculating binding

155 free energy. The individual contributions of protein residues to the three energetic components

156   were determined through per-residue decomposition. The temperature used for Poisson–

157   Boltzmann calculation was set to 300K.

158   Prediction of ADME by Computational analysis

159   ADME analysis of Bisdemethoxycurcumin, Demethoxycurcumin, and Diferuloylmethane at pH

160   7 was examined using online software tools [27]. The important parameters related to ADME

161   properties such as Proudfoot's rule of five, pharmacokinetic properties, drug likeliness, molar

162   refractivity, and solubility of the drug was deliberated [28].

163

164

165

166

167

168

169

170

171

172

173

174

175

176

177

178

179

180

181

Discussion

Until now, no specific antiviral medication was discovered for COVID-19 the only control measure includes proper hand washing, social distancing, mouth and nose masking, travel restriction, and infected person isolation [1 2 4]. Furthermore, Scientists around the world are developing many potential vaccines for COVID-19 and the biggest vaccination campaign in history is underway. However, according to the world meter report, the coronavirus COVID-19 is still affecting 219 countries and worldwide 160 686 749 peoples infected and 3335 948 people died until May 14, 2021, 20:04 GMT. In the context of Ethiopia, this virus died about 3,951 people and infected 264,960 people. Viruses continually change through mutations and the gene encoding the S protein of SARS-CoV-2, various mutations have been reported and recently, the United Kingdom (UK) (VOC-202012/01 or VUI-202012/01 or B.1.1.7), Indian (B.1.617) and South Africa (501Y.V2 or 20C/501Y.V2B.1.351) have faced a rapid increase in COVID-19 mediated by new variants [48 49]. One way of recovering from this problem could be to identify potent COVID-19 inhibitors is urgently needed, as the situation getting worst. In this regard, plants serve as the source of therapeutic ingredients in the history of the human race. As far as we know, little previous research has investigated curcumin sp polyphenols inhibitory effect on COVID-19. Curcumin consists of three major compounds, namely, diferuloylmethane (60–70%), demethoxycurcumin (20–27%), and Bisdemethoxycurcumin (10–15%) [29 30]. The review showed curcumin derived polyphenols exhibit antiviral activity for influenza, hepatitis C virus, HIV virus, anti-inflammatory, antibacterial, and antioxidant properties and also exert substantial anti carcinogenic activities [29 30 31]. Wet lab experimental approaches for the study of interactions between therapeutic substance and target proteins are not cheap, not safe, labors, and time-consuming [32 33]. There are many alternative methods are available for solving these problems. In this study, we proposed the combinational strategy of docking and molecular dynamics simulation. A series of recent studies have indicated that combinational strategy of the docking and molecular dynamic simulations techniques identify the targets for several bioactive compounds whose in vivo targets are unknown including COVID-19 [38 40 41]. The aim of this study is to investigate the binding affinity of three Curcumin derived polyphenols against COVID-19 the main protease (Mpro) binding pocket (Mpro) and the identification of important residues for interaction with curcumin derived polyphenols. For this purpose, we used protein-carmofur (PDB code: 7BUY) as a model to offer evidence that could elucidate the mechanisms

213   of curcumin sp polyphenols inhibition. At the beginning of this study, curcumin sp-derived

214   polyphenols were subjected to ADMETox evaluation. According to Proudfooti's rule states that

215   for any compound to be selected as a potential drug it should have; molar refractivity between 40

216   and 130, Less than 10 hydrogen bond acceptors, less than 5 hydrogen bond donors, high

217   lipophilicity (expressed as LogP ≤5) and Molecular mass < 500 Dalton. Therefore, three selected

218   curcumin sp-derived polyphenols used in this study passed all the five criteria mentioned in

219   Proudfoot's rule (Table 3 supp.). Demethoxycurcumin and bisdemethoxycurcumin polyphenol

220   passed the ADME evaluation and throughout the screening, only Diferuloylmethane passed the

221   predicted toxicity evaluation. Thus this study suggests that these phytochemicals have the

222   potential to work effectively as drugs. Next, to validate our docking methodology crystal

223   structure of COVID-19 main protease binding pocket (Mpro) (PDB code: 7BUY) with carmofur

224   bound at the binding pocket was retrieved from PDB and re-dock with carmofur. The values of

225   the RMSD between the Mpro crystals structure (RMSD 1.6) and the re-dock structures (RMSD

226   1.9) confirmed close-match between docked and original structure. This confirmed our model

227   structure is good quality and continued docking our work. Molecular docking studies showed

228   that curcumin polyphenols have binding energy values between −12.17 to −12.32 kcalmol^{-1} as

229   shown in table 1 (Table 1). Recent theoretical developments have revealed that Docking studies

230   on different traditional medicine inhibitors activity for the SARS-CoV-2 protease. Several

231   studies have been reported the binding energy of molecules less than or/and higher values

232   compared to this study. Cherrak et al. reported in the literature that Quercetin-3-O-rhamnoside

233   showed the highest binding affinity -7kcal/mol^{-1} [34]. Moreover, it was observed that curcumin

234   exhibited the highest binding free energy of −18.21 kcal/mol^{-1} in different COVID-19 main

235   protease, which is targeted in this study [35]. And also, docking of SARS-CoV-2 spike protein

236   (PDB ID: 6LU7) with nelfinavir, lopinavir, kaempferol, quercetin,luteolin-7-

237   glucoside,demethoxycurcumin, naringenin, apigenin-7-glucoside, oleuropein, curcumin, catechin,

238   epicatechin-gallate, gingerol, gingerol, and allicin binding energies ranges between -4.03 to -7.6

239   kcal/mol^{-1} [36]. Recently, Computational docking of 14 compounds representing flavonoids,

240   phenolic acids and terpenes from honey and propolis with two different targets from COVID-19

241   showed binding affinity ranges between −5.6 to −7.8 kcal/mol^{-1} [48]. Bisdemethoxycurcumin,

242   Demethoxycurcumin and Diferuloylmethane revealed a minimum of two hydrogen bonds and a

243   maximum of three hydrogen bonds for the Mpro binding pocket of SARS-CoV-2 (Table 1). In

244 line with previous studies, hydrogen bonds are the most important bonds in determining the

245 binding affinity, selectivity, and stabilization effect of curcumin derived polyphenols with Mpro

246 [37]. The inhibition constant (Ki) is higher for Demethoxycurcumin (281.22uM) than

247 Bisdemethoxycurcumin (98.83uM) and Diferuloylmethane (156.42uM) as shown in table 1.

248 Prior research suggests that the smaller the Ki, the greater the binding affinity and the smaller

249 amount of medication needed to inhibit the activity of that enzyme [33]. The RMSD values

250 obtained for the lowest-energy poses predicted for each polyphenol are shown in Table 1 and

251 average RMSD results ranging from 57.0 to 70.0 Å RMSD. But this is not relevant data for this

252 study.

253 Furthermore, residues forming stable contact with polyphenols include Phe294, Gln110, Gln240,

254 Gln192 Asn142, Lys137, Thr199, and Leu272 with probabilities larger than 85% (Figure 1 table

255 1). Bisdemethoxycurcumin and Demethoxycurcumin have lost hydrophobic interaction with

256 Pro293 with Tyr239, respectively (figure 1). Besides this, a total of eight residue pairs that have

257 average distances smaller than 10.0Å within free enzyme residues and Mpro-polyphenols

258 complexes binding pocket residues and surface residues reported (Table 2). This implies that

259 residue from both surface and binding pocket protein is involved in direct contact with curcumin

260 derived polyphenols. Furthermore, the inter-residue distances between the binding pocket and

261 surface residues in Mpro-bisdemethoxycurcumin and Mpro-demethoxycurcumin complex are

262 slightly different from that of Mpro-diferuloylmethane, particularly for Pro252/Lys137,

263 Thr292/Thr199, Ile200/Leu272, and Arg188/Phe294 residues (Table 2). In line with previous

264 studies, residue serine interacts with residue Phe140 and Glu166 to stabilize the enzyme-

265 polyphenols complex binding site [7]. For residues Gln192, Leu167, Ser144, Gly143, His114,

266 Pro168, His41, and Cys145, their contact probabilities with bisdemethoxycurcumin were

267 increased significantly and Cys145 is a key catalytic residue which is consistent with a previous

268 study [7]. Residues forming stable contact with polyphenol include Phe294, Gln110, Gln240,

269 Gln192 Asn142 Lys137 Thr199, and Leu272 the complexes with probabilities larger than 85%

270 (Figure 1). Also, for residues Glu288, Asp289, Leu287 Arg131, Tyr239, Leu271, Asn274,

271 Gly275, and Leu286 the probabilities of contacts between demethoxycurcumin increased

272 significantly after binding and they also form stable contacts (figure 1). For residues Arg188,

273 Val202, Gly109, Pro293, Ile249, Pro252, Thr292, Ile200, and Cys145 their contact probabilities

274 with bisdemethoxycurcumin were increased significantly and Cys145 is a key catalytic residue

275 which is consistent with a previous study [7]. Pro168, His41 and Val116 residues contact

276 probabilities between demethoxycurcumin-Mpro and bisdemethoxycurcumin-Mpro decreased

277 (Table 3). Previous studies have shown COVID-19 main protease possesses a dynamic binding

278 pocket loop comprising domain-I (residues 10 to 99) and domain-II (residues 100 to 184), in

279 which most of the residues in this study laid [7 42 43].

280 To examine the stability and conformational dynamics of the Mpro–three curcumin derived

281 polyphenols complex and free Mpro, we calculated the RMSD for the backbones of all residues

282 (Figure 1; Figure 2). In this study, much attention has been given to the impact of curcumin

283 derived polyphenols diferuloylmethane, demethoxycurcumin, and bisdemethoxycurcumin on the

284 structure and dynamics of the main protease (Mpro). Here free Mpro has a significantly large

285 root-mean-square deviation compare to curcumin sp polyphenols binding the Mpro pocket

286 domain. The time evolution plot of RMSD displays the complex structure of diferuloylmethane-

287 Mpro, demethoxycurcumin-Mpro, and bisdemethoxycurcumin-Mpro attain equilibrium at

288 1000ps and remains stable up to 5000ps (Figure 1). In particular, the complex structure with

289 demethoxycurcumin and bisdemethoxycurcumin is largely stabilized around 3000ps to 6000ps

290 (Figure 2). Likewise, its fluctuation main protease complex is smaller, especially in the segment

291 Asn226 to Gly252, which is the active-site loop region which is consistent with the previous

292 study discussed (Figure 3). Particularly, binding of the bisdemethoxycurcumin was observed to

293 decrease RMSF of some segments (30 to 100, 200 to 250, and 250 to 300) and increase that of

294 the segment (100 to 150) (Figure 3). The higher value of RMSF depicted that the structure has

295 some flexible regions while the lower value of RMSF indicated that the structure was good in

296 terms of secondary structure [22]. Therefore, the result revealed the interactive stabilizing effect

297 of Demethoxycurcumin and Bisdemethoxycurcumin. Also, the impact of these polyphenols on

298 the structure and dynamics of the Main protease binding pocket domain region was further

299 regulated by a hydrogen bond. Here, we also examine the time evolution of hydrogen bond (H-

300 bond) formed between the Mpro and curcumin sp derived polyphenols (Figure 4). We found that

301 the trajectory of bisdemethoxycurcumin revealed five H-bonds with Mpro, three H-bonds were

302 seen consistently during the simulation (Figure 4). Demethoxycurcumin revealed the presence of

303 ten H-bonds with Mpro but, three H-bond can be seen retained throughout the simulation, the H-

304 bond plot of diferuloylmethane shows a maximum of seven H-bond interactions with Mpro, but

305 only two seen retained throughout the simulation (Figure 4), while the carmofur showed the

306   lesser number of hydrogen bonds [7]. The strong hydrogen bonding interactions between the
307   demethoxycurcumin-Mpro and bisdemethoxycurcumin-Mpro may be a potential inhibitor [21].
308   This study may contribute to the understanding of the structure-based design of COVID-19
309   therapy with curcumin derived polyphenols. Future investigations are necessary to validate the
310   kinds of conclusions that can be drawn from this study.

311   **Conclusions**

312   Until now, Great progress has been made in Computational methods involving drug target
313   identification in a paradigm change in both industry and academics. Computational techniques,
314   for example, data mining, homology modeling, MD simulation, cheminformatics, docking, and
315   QSAR modeling have provided powerful techniques for target identification, drug discovery, and
316   optimization. First, curcumin derived polyphenols were subjected to in silico ADMETox and we
317   found the potential ability to work effectively as drugs. Based on the results of the present study,
318   it can be concluded that the investigated curcumin derived polyphenols could interfere with the
319   important residues in the enzymatic binding pocket to inhibit the main protease enzyme COVID-
320   19 virus. Demethoxycurcumin and bisdemethoxycurcumin polyphenols are identified to have
321   inhibitory activities against novel COVID-19 main protease. Bisdemethoxycurcumin has a
322   stronger bond and high affinity with the Main protease (Mpro). Furthermore, the average RMSD
323   values of the backbone atoms in docked curcumin sp derived polyphenols were calculated from
324   10000ps and showed stable RMSD values between 1nm to 2nm for Bisdemethoxycurcumin and
325   Demethoxycurcumin at the reasonably consistent temperature (~300 K) and pressure (1bar),
326   whereas diferuloylmethane complex showed RMSD value between 5.5 and 6.2 with same cut-off
327   parameters. These data validated that the docked Mpro-Bisdemethoxycurcumin complexes and
328   Mpro-Demethoxycurcumin complexes are more stable than the Mpro-diferuloylmethane
329   complex. To completely investigate the effects of curcumin derived polyphenols, this study
330   recommended the roles of polyphenols identified for further exploration in a wet lab experiment.

331   **Acknowledgement**

332   For the success of this work we would like to acknowledge effort of our family for their
333   inspiration. We acknowledge the university of Addis Ababa Science and Technology for using
334   computational resources.

335

336 **References**

337 **1.** World Health Organization. (2020). Coronavirus Disease 2019 (COVID-19) Situation Report
338 –43. 2020. Available online: https://www.who.int/emergencies/diseases/novel-coronavirus-
339 2019/situation-reports

340 **2.** Guarner J. (2020). Three emerging coronaviruses in two decades: the story of SARS, MERS,
341 and now COVID-19. *American Journal of Clinical Pathology*; 153: 420–421.

342 **3.** Chen Y, Liu Q and Guo D. (2020). Emerging coronaviruses genome structure, replication and
343 pathogenesis. *J Med Virol*; 92(10):2249.

344 **4.** Zhao Q, Weber E & Yang H. (2013). Recent developments on coronavirus main protease/3C
345 like protease inhibitors. *Recent Patents on anti-Infective Drug Discovery*; 8(2): 150–156.

346 **5.** Pal M, Berhanu G, Desalegn C and Kandi V. (2020).Severe Acute Respiratory Syndrome
347 Coronavirus-2 (SARS-CoV-2): An Update. *Cureus*; 12(3): e7423.

348 **6.** Woo PCY, Huang Y, Lau SKP and Yuen KY. (2010). Coronavirus Genomics and
349 Bioinformatics Analysis. Viruses; 2(8):1804–20.

350 **7.** Jin Z, Zhao Y, Sun Y, Zhang B, Wang H, Wu Y, Zhu Y, Zhu C, Hu T, Du X, Duan Y *et al*.
351 (2020). Structural basis for the inhibition of SARS-CoV-2 main protease by antineoplastic drug
352 Carmofur. Nature structural and molecular biology; 27: 529–532

353 **8.** Muralidharan N, Sakthivel R, Velmurugan D & Gromiha MM. (2020). Computational studies
354 of drug repurposing and synergism of lopinavir, oseltamivir and ritonavir binding with SARS-
355 CoV-2 protease against COVID-19. *Journal of Biomolecular Structure and Dynamics*; 16; 1-6.

356 **9.** Liu X, Zhang B, Jin Z, Yang H, Rao Z. (2020). The Crystal Structure of COVID-19 Main
357 Protease in Complex with an Inhibitor N3. *J. Chem. Inf. Model*; 60 (7): 3593–3602

358 **10.** WHO Director-General's opening remarks at the media briefing on COVID-19 - 3 March
359 2020 - World Health Organization, March 3, 2020

360 **11.** Islam MT, Khan MR & Mishra SK. (2019). An updated literature-based review:
361 Phytochemistry, pharmacology and therapeutic promises of Nigella sativa L. *Oriental Pharmacy*
362 *and Experimental Medicine*; 19(2): 115–115.

363 **12.** Forni C , Facchiano F, Bartoli M, Pieretti S, Facchiano A, D'Arcangelo D, Norelli S, Valle
364 G, Nisini R, Beninati S, Tabolacci C & Jadeja RN. (2019). Beneficial Role of Phytochemicals on

365 Oxidative Stress and Age-Related Diseases. *BioMed Research International*: 2019(4, article

366 918).

367 **13.** Hatcher H, Planalp R, Cho J, Torti FM and Torti SV. Curcumin: from ancient medicine to

368 current clinical trials. *Cell Mol Life Science*; 65(11):1631–52.

369 **14.** Anbarasu K and Jayanthi S. (2018). Identification of curcumin derivatives as human LMTK3

370 inhibitors for breast cancer: a docking, dynamics, and MM/PBSA approach, *Springer*; 8(5):228-

371 239.

372 **15.** Mounce BC, Cesaro T, Carrau L, Vallet T & Vignuzzi M. (2017). Curcumin inhibits Zika

373 and chikungunya virus infection by inhibiting cell binding. Antiviral Research; 142: 148–157.

374 **16.** Praditya D, Kirchhoff L, Bruning J, Rachmawati H, Steinmann J & Steinmann E. (2019).

375 Anti-infective properties of the golden spice curcumin. *Frontiers in Microbiology*; 10: 912.

376 **17.** Anandakrishnan R, Aguilar B and V. Onufriev A. (2012). H++ 3.0: automating pK

377 prediction and the preparation of biomolecular structures for atomistic molecular modeling and

378 simulation. *Nucleic Acids Res*; 4: 537-541.

379 **18.** Benkert P, Michael K, Torsten S. (2009). QMEAN server for protein model quality

380 estimation. *Nucleic Acids Res*; 37:510–514

381 **19.** Colovos C and Yeates TO. (1993).Verification of protein structures: patterns of nonbonded

382 atomic interactions. *Protein Science*; 2(9):1511-9.

383 **20.** Pontius J, Richelle J and Wodak SJ. (1996). Deviations from standard atomic volumes as a

384 quality measure for protein crystal structures. *J Mol Biol*; 264(1):121-36.

385 **21.** Bolton EE, Wang Y, Thiessen PA and Bryant SH. (2008). PubChem: integrated platform of

386 small molecules and biological activities. Annual Reports in Computational Chemistry. *Elsevier*;

387 4(2008): 217–241.

388 **22.** O'Boyle, NM, Banck M, James CA, Morley C, Vandermeersch T & Hutchison GR. (2011).

389 Open Babel: An open chemical toolbox. Journal of Cheminformatics; 3(1):33.

390 **23.** Morris GM, Huey R, Lindstrom W, Sanner MF, Belew RK, Goodsell DS, Olson AJ. (2009).

391 AutoDock4 and AutoDockTools4: Automated docking with selective receptor flexibility. *J

392 Comput Chem*; 30(16):2785-91.

393 **24.** Nelson M, Humphrey W, Gursoy A, Dalke A, V.Kalé L, D. Skeel R and Schulten K. (1996).

394 NAMD - A parallel, object-oriented molecular dynamics program. *International Journal of

395 Supercomputer Applications and High Performance Computing*; 10:251-268.

396 **25.** Vanommeslaeghe K, Raman EP and MacKerell AD. (2012). Automation of the CHARMM

397 General Force Field (CGenFF) II: assignment of bonded parameters and partial atomic charges.

398 *Journal of chemical information and modeling*; 52 (12): 3155-3168.

399 **26.** Kumari R, Kumari R & Lynn A. (2014). g_mmpbsa--a GROMACS tool for high throughput

400 MM-PBSA calculations. *J Chem Inf Model*; 54(7):1951-1962.

401 **27.** B. Baell J and A. Holloway G. (2012). New Substructure Filters for Removal of Pan Assay

402 Interference Compounds (PAINS) from Screening Libraries and for Their Exclusion in

403 Bioassays. *J. Med. Chem*; 53 (7): 2719–2740.

404 **28.** Daina A, Michielin O & Zoete V. (2017). SwissADME: a free web tool to evaluate

405 pharmacokinetics, drug-likeness and medicinal chemistry friendliness of small molecules. *Sci.*

406 *Rep*; 7:42717.

407 **29.** Heger M, van Golen RF, Broekgaarden M and Michel MC. (2013). The molecular basis for

408 the pharmacokinetics and pharmacodynamics of curcumin and its metabolites in relation to

409 cancer. Pharmacological Reviews; 66(1):222-307

410 **30.** Nelson KM, Dahlin JL, Bisson J, Graham J, Pauli GF and Walters MA. (2017). The essential

411 medicinal chemistry of curcumin. J Med Chem; 60(5):1620–1637.

412 **31.** Praditya D, Kirchhoff L, Brüning J, Rachmawati H, Steinmannand J and Steinmann E.

413 (2019). Anti-infective Properties of the Golden Spice Curcumin. Front Microbiol; 10: 912.

414 **32.** SARBASHRI BANK. (2020). In-silico analysis of potential interaction of drugs and the

415 SARS-CoV-2 spike protein. Research square. DOI: https://doi.org/10.21203/rs.3.rs-30401/v1

416 **33.** Bachmann KA and Lewis JD. (2005). Predicting inhibitory drug-drug interactions and

417 evaluating drug interaction reports using inhibition constants. Ann Pharmacother; 39:1064-72.

418 **34.** Cherrak SA, Merzouk H and Mokhtari-Soulimane N. (2020). Potential bioactive

419 glycosylated flavonoids as SARS-CoV-2 main protease inhibitors: A molecular docking and

420 simulation studies. *Plos One*; 15 (10), e0240653. doi:10.1371/journal.pone.0240653

421 **35.** Adeoye A. (2020). Pharmacoinformatics and hypothetical studies on allicin, curcumin, and

422 gingerol as potential candidates against COVID-19-associated proteases. *Journal of*

423 *biomolecular Structure & Dynamics*. DOI: 10.1080/07391102.2020.1813630

424 **36.** Khaerunnisa S, Kurniawan H, Awaluddin R, Suhartati S and Soetjipto S. (2020). Potential

425 Inhibitor of COVID-19 Main Protease (Mpro) from Several Medicinal Plant Compounds by

426   Molecular   Docking   Study.   *Hindawi*;   Volume   2020 |Article   ID   6307457 |

427   https://doi.org/10.1155/2020/6307457

428   **37.** Baby K, Maity S, Mehta CH, Suresh A, Nayak UY and Nayak Y. (2020). Targeting SARS-

429   CoV-2 main protease: a computational drug repurposing study. *Archives Medical Res*. 52 (1),

430   38–47. doi:10.1016/j.arcmed.2020.09.013

431   **38.** Rahman MS, Hoque MN, Islam MR, Akter S, Rubayet U, Alam ASM, Siddique MA, Saha

432   O, Rahaman MM, Sultana M, Crandall KA and Hossain MA. (2020). Epitope-based chimeric

433   peptide vaccine design against S, M and E proteins of SARS-CoV-2, the etiologic agent of

434   COVID-19 pandemic: an in silico approach. *PeerJ* 8:e9572 https://doi.org/10.7717/peerj.9572

435   **39.** Hoque MN, Chaudhury A, Akanda MAM, Hossain MA and Islam MT. (2020). Genomic

436   diversity and evolution, diagnosis, prevention, and therapeutics of the pandemic COVID-19

437   disease. *PeerJ* 8:e9689 https://doi.org/10.7717/peerj.9689

438   **40.** Fiesco-Sepúlveda KY and Serrano-Bermúdez LM. (2020). Contributions of Latin American

439   researchers in the understanding of the novel coronavirus outbreak: a literature review. *PeerJ;*

440   8:e9332 https://doi.org/10.7717/peerj.9332

441   **41.** Cortés-García CJ, Chacón-García L, Mejía-Benavides JE and Díaz-Cervantes E. (2020).

442   Tackling the SARS-CoV-2 main protease using hybrid derivatives of 1, 5-disubstituted tetrazole-

443   1,   2,   3-triazoles: an   in   silico   assay.   *PeerJ*;   Physical   Chemistry   2:e10

444   https://doi.org/10.7717/peerj-pchem.10

445   **42.** Kouznetsova VL, Zhang A, Tatineni M, Miller MA and Tsigelny IF. (2020). Potential

446   COVID-19 papain-like protease PLpro inhibitors: repurposing FDA-approved drugs. *PeerJ*;

447   8:e9965 https://doi.org/10.7717/peerj.9965

448   **43.** Kandeel M, Kitade Y and Almubarak A. (2020). Repurposing FDA-approved

449   phytomedicines, natural products, antivirals and cell protectives against SARS-CoV-2 RNA-

450   dependent RNA-polymerase. *PeerJ*; 8:e10480 https://doi.org/10.7717/peerj.10480

451   **44.** Elaswad A, Fawzy M, Basiouni S and Shehata A. (2020). Mutational spectra of SARS-CoV-

452   2 isolated from animals. *PeerJ*; 8:e10609 https://doi.org/10.7717/peerj.10609

453   **45.** Parlikar A, Kalia K, Sinha S, Patnaik S, Sharma N, Vemuri SG and Sharma G. (2020).

454   Understanding genomic diversity, pan-genome, and evolution of SARS-CoV-2. *PeerJ;* 8:e9576

455   https://doi.org/10.7717/peerj.9576

456   46. Bin Emran T, Rahman MA, Nasir Uddin MM, Dash R, Firoz Hossen M, Mohiuddin M and

457   Rashadul Alam m. (2015). Molecular docking and inhibition studies on the interactions of

458   Bacopa monnieri's potent phytochemicals against pathogenic Staphylococcus aureus. *DARU*

459   *Journal of Pharmaceutical Sciences*; 23(1): 1-8

460   47. Dash R, Bin Emran T, Nasir Uddin MM, Islam A and Junaid M. (2014). Molecular docking

461   of fisetin with AD associated AChE, ABAD and BACE1 proteins. *Bioinformation*; 10(9): 562

462   48. Dawood AA. (2020). Mutated COVID-19 may foretell a great risk for mankind in the future.

463   *New Microbes New Infect*; 35:100673.

464   49. Korber B, Fischer WM, Gnanakaran S, Yoon H, Theiler J, Abfalterer W, Hengartner N,

465   Giorgi EE, Bhattacharya T, Foley B *et al*. (2020).Tracking Changes in SARS-CoV-2 Spike:

466   Evidence that D614G Increases Infectivity of the COVID-19 Virus. Cell; 182:812–827.e19.

467

Figure 1

Figure 1. Plots of Root-mean-square deviations of free SARS CoV-2 main protease (Mpro) (Blue) and the complex of SARS CoV-2 main protease (7BUY) (Red) with three polyphenols along the MD simulation time

(A) free SARS CoV-2 main protease (Mpro) (Blue)

(B) the complex of SARS CoV-2 main protease (7BUY) (Red) with three polyphenols
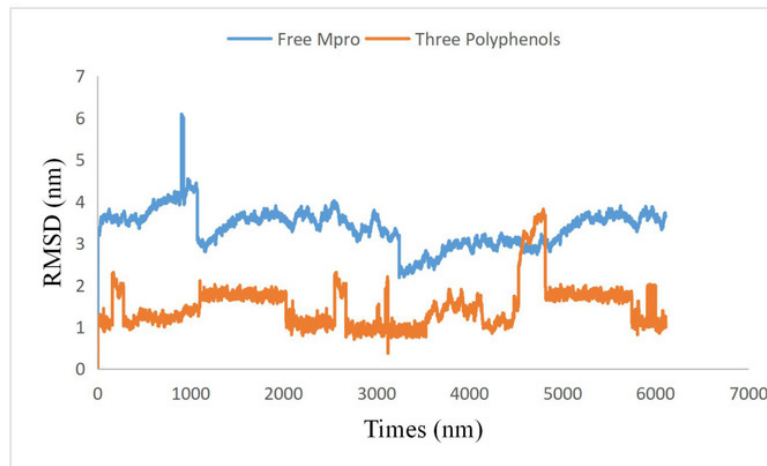
Figure 2

Figure 2. Plots of Root-mean-square deviations of free main CoV-2 protease (Mpro) (Gray) and the complex of Mpro with Bisdemethoxycurcumin (Yellow), Demethoxycurcumin (Blue) and Diferuloylmethane (Red) along the MD simulation time for three individual pol

(A) free main CoV-2 protease (Mpro) (Gray) and the complex of Mpro with

Bisdemethoxycurcumin (Yellow), (B) Demethoxycurcumin (Blue) and (C) Diferuloylmethane

(Red)
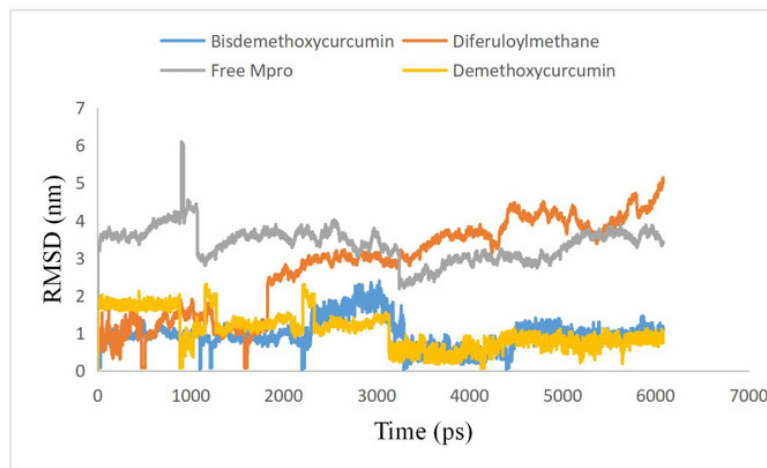
Figure 3

Figure 3. RMSF plot of free main CoV-2 protease (Mpro)(Yellow) and the complex of Mpro with Bisdemethoxycurcumin (Red), Demethoxycurcumin (Blue) and Diferuloylmethane (Gray) along the MD simulation time for three individual polyphenols.

(A) free main CoV-2 protease (Mpro)(Yellow) and (B) the complex of Mpro with

Bisdemethoxycurcumin (Red), (C) Demethoxycurcumin (Blue) and (D) Diferuloylmethane
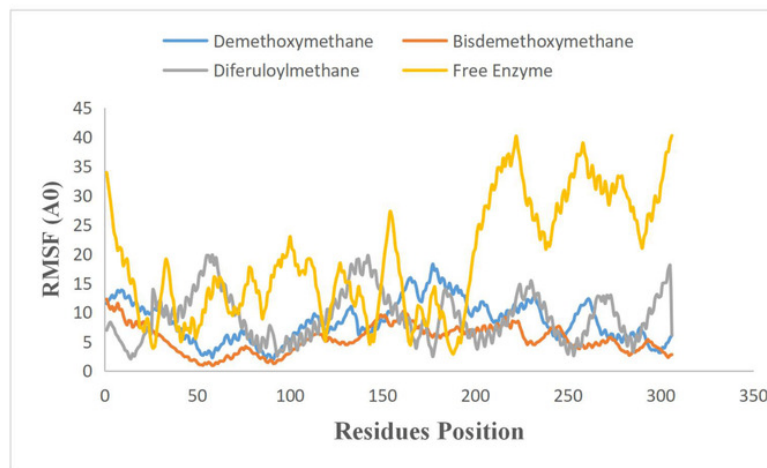
(Gray)

Figure 4

Figure 4. Number of hydrogen bond present in Bisdemethoxycurcumin-SARS-CoV-2 main protease (Yellow), Demethoxycurcumin-SARS-CoV-2 main protease (Gray), free SARS-CoV-2 main protease (Red) and diferuloylmethane-main protease (Blue).

(A) Bisdemethoxycurcumin-SARS-CoV-2 main protease (Yellow), (B) Demethoxycurcumin-SARS-CoV-2 main protease (Gray), (C) free SARS-CoV-2 main protease (Red) and (D) diferuloylmethane-main protease (Blue).
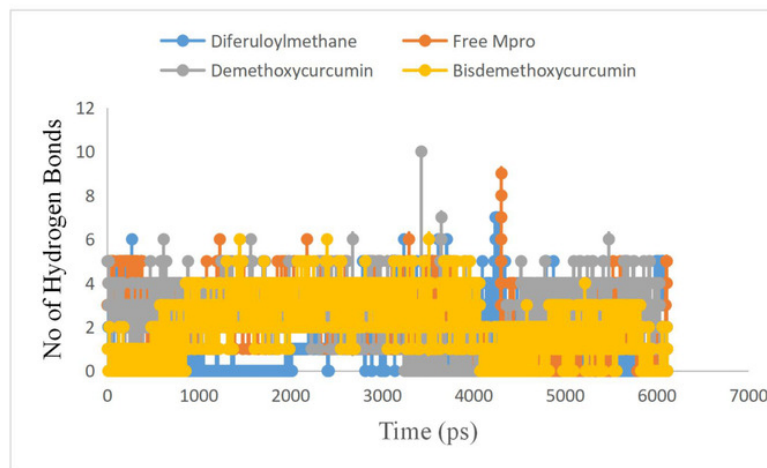
Table 1 shows molecular docking results to determine the SARS CoV-2 main protease (Mpro) binding pocket affinity towards selected curcumin sp derived polyphenols at 298.15 K

Protein-ligand complexes	Binding Energy (kcal/mol)	Inhibition Constant (Ki) (uM)	RMSD [b] (A⁰)	Residues involved in interaction	No of Hydrogen Bonds
Diferuloylmethane - COVID-19 main protease	-12.25	156.42	70.645	Asn142 and Gln192	2
Demethoxycurcumin -COVID-19 main protease	-12.17	281.22	57.842	Leu272, Thr199,Lys137	3
Bisdemethoxycurcumin-COVID-19 main protease	-12.32	98.83	65.030	Phe294, Gln110 and Glu240	3

Table 2 Inter-residue distances and corresponding standard deviations. In each residue pair, one belongs to the binding pocket loop region and the other belongs to surface part of the enzyme

Residues	Free enzyme	Enzyme-Demethoxycurcumin complex	Enzyme-Bisdemethoxycurcumin complex
Arg188- Phe294	5.154 ± 1.531	5.937 ± 1.604	4.5 ± 1.10
Val202- Gln110	9.419 ± 1.440	8.455 ± 1.090	9.25 ± 1.440
Gly109- Gln240	10.111 ± 1.838	8.296 ± 1.459	11.31 ± 1.14
Pro293- Gln192	8.570 ± 1.663	7.095 ± 1.022	5.13 ± 1.04
Ile249- Asn142	9.170 ± 5.015	10.485 ± 1.560	6.71 ± 0.44
Pro252- Lys137	7.11 ± 0.02	8.5 ± 1.4	5.63 ± 1.04
Thr292- Thr199	5.109 ± 0.440	6.039 ± 0.940	4.110 ± 0.230
Ile200- Leu272	7.213 ± 0.018	9.216 ± 0.218	6.121 ± 0.618

Table 3 residues forming contacts with diferuloylmethane polyphenol, demethoxycurcumin polyphenol and bisdemethoxycurcumin polyphenol in binary complexes.

Residues	Enzyme-Demethoxycurcumin complex	Enzyme Bisdemethoxycurcumin complex	Enzyme-diferuloylmethane complex
Gln192	0.70 ± 0.01	0.85 ± 0.01	0.45 ± 0.02
Leu167	0.90 ± 0.03	0.98 ± 0.004	0.60 ± 0.05
Tyr239	0.60 ± 0..07	0.80 ± 0.01	0.30 ± 0.01
Asp289	0.70 ± 0.19	0.90 ± 0.004	0.60 ± 0.1
Arg188	0.75 ± 0.011	0.80 ± 0.05	0.73 ± 0.09
Glu166	0.80 ± 0.04	0.80 ± 0.01	0.90 ± 0.01
Glu288	1.00 ± 0.06	0.50 ± 0.01	0.60 ± 0.12
His114	1.00 ± 0.00	1.00 ± 0.00	0.50 ± 0.03
Gln189	0.70 ± 0.05	0.90 ± 0.00	1.00 ± 0.09
Pro168	0.30 ± 0.01	1.00 ± 0.00	0.85 ± 0.05
Gln189	0.45 ± 0.02	1.00 ± 0.00	0.40 ± 0.16
Cys145	0.75 ± 0.09	0.90 ± 0.01	0.60 ± 0.06
Met165	0.80 ± 0.1	0.85 ± 0.12	0.50. ± 0.12
His 164	0.40 ± 0.00	0.70 ± 0.01	1.00 ± 0.04
Asp187	0.90 ± 0.03	0.90 ± 0.03	0.90 ± 0.03
Arg188	0.93 ± 0.12	0.89 ± 0.01	0.76 ± 0.23